Research Article

Journal of Scientific Enquiry
Vol: 5, Pages: 119-131

Tuning of structural, optical properties of CdS nanoparticles with incorporation of Arjuna bark extract as capping reagent

Parimal Tudu[1], Moinur Rahaman[1], Shivsankar Dey[1], Rittwick Mondal[1], Soumyajoyti Kabi[2], Ardhendu Sekhar Patra[1,*] and Sonjoy Mondal[1,*]

[1]*Department of Physics, Sidho-Kanho-Birsha University, Purulia-723104, India*
[2]*Department of Physics, Hijli College, Kharagpur 721306, India*
*Corresponding Authors. E-mail address: sanjoy-mandal@skbu.ac.in

Received: 18.09.2025; Accepted: 01.11.2025; Published online: 31.12.2025
DOI: `https://doi.org/10.54280/jse.255108`

Abstract: This research paper explores a sustainable and environmentally friendly approach to synthesize cadmium sulfide (CdS) nanoparticles utilizing a biogenic source such as Arjuna Bark as a capping reagent through a green synthesis process. The research focuses on the role of bioelements in controlling the size, morphology, and stability of the nanoparticles. Characterization techniques, including UV-visible spectroscopy, XRD, FTIR, PL, and Raman spectroscopy, are used to explain the structural, optical and chemical properties of the CdS nanoparticles synthesized through this green approach. The crystalline cubic phase of these newly synthesized CdS NPs are identified by using Debye-Scherer's equation, corresponding to (111), (220), (311) planes respectively. It is found that the crystalline sizes vary with different mol%. The optical band gap energies are estimated by deploying the Tauc plot, which decreases from 4.49 eV to 3.82 eV with different doping concentrations, affirming the semiconducting nature of the synthesized samples. The density functional theory (DFT) study supports the experimentally observed trend in band gap values and provides insight into the electronic structure of the synthesized CdS nanoparticles. Furthermore, the paper delves into the potential applications of these newly synthesized CdS nanoparticles, highlighting the eco-friendliness and biocompatibility aspects of this green synthesis process.

Key words: FTIR spectroscopy; PL study; Biogenic Sources; DFT; Band gap energy.

1 Introduction

In view of the amazing size-dependent features that appear at the nanoscale and the constantly growing range of real-world applications that these materials permit, nanoparticle engineering has quickly developed into a key component of contemporary nanotechnology [1–3]. Cadmium sulphide (CdS), an II–VI semiconductor with a direct band gap of ≈2.4 eV at room temperature, is one of the many classes of nanosystems currently being studied [4]. It has emerged as a model material because of its exceptional photocatalytic activity, high extinction coefficient, excellent electron mobility, and easily adjustable quantum confinement effects [5–7]. CdS has found prominent roles in next-generation semiconductor components [8-9], energy conversion and storage devices [10-11], high efficiency solar cells [12–14], light emitting and photodetector architectures [15], and emerging biomedical arenas like targeted drug delivery, antimicrobial coatings, and theranostics [16–18] due to its precise modulation of its optoelectronic response by simply adjusting particle size. CdS is a desirable platform for label-free biosensor development, enzyme activity tests, and point-of-care diagnostics due to its potent size-dependent fluorescence and photostability [19–23]. While many metallic nanoparticles have been investigated for similar applications [24–26], chalcogenide nanocrystals like CdS, ZnS, and PbS are often preferred for a number

of strong reasons [27–29]. Firstly, without the requirement for intricate alloying, their band gaps can be precisely adjusted across the UV–NIR spectrum through simple adjustment of particle size or composition, allowing for application-specific optical and electrical tailoring. Secondly, in a broad variety of pH, temperature, and ionic strength conditions, they preserve crystallinity and functional performance because to their exceptional environmental and colloidal stability. Third, chalcogenides exhibit high quantum yields, and intrinsically strong photoluminescence features essential for luminous labelling, multiplexed imaging, and single particle tracking. Furthermore, accessible bottom-up synthesis strategies provide accurate control over defect density, surface chemistry, and shape while still being affordable and compatible with green chemistry approaches. Subsequently, compared to many heavy metal substitutes, appropriately capped CdS and related chalcogenide nanocrystals show encouraging biocompatibility and a lower ecological effect, increasing their applicability in environmental and therapeutic applications. Chalcogenide nanoparticles are a flexible, ever-developing platform at the nexus of materials science, physics, chemistry, and biotechnology because of these combined characteristics. CdS and its congeners are still at the forefront of nanoscience research and application because of their exceptional capacity to connect basic science with real-world innovation. For their specific benefits, cadmium sulphide (CdS) nanoparticles are utilized more frequently than zinc sulphide (ZnS) and lead sulphide (PbS) nanoparticles in some applications. ZnS is less helpful in several optoelectronic applications than CdS due to its larger bandgap. Contrarily, CdS has an adjustable bandgap, which makes it very beneficial for solar cells and photodetectors [30]. Additionally, CdS nanoparticles exhibit exceptional photocatalytic properties, especially in the visible light spectrum, which is advantageous for uses including environmental remediation and water purification [31]. Compared to CdS nanoparticles, ZnS and PbS nanoparticles can be more challenging to control in terms of size and properties, and they may require more advanced methods. Additionally, CdS nanoparticles exhibit excellent photoluminescence, which makes them advantageous for fluorescent labelling and light-emitting diodes (LEDs) [32].

Traditional methods for CdS nanoparticle synthesis involve the use of hazardous chemicals and toxic reagents which have raised concerns regarding environmental sustainability and human health. As a response to these concerns, the concept of green synthesis, utilizing eco-friendly and biocompatible materials, has emerged as a promising approach [33]. Green synthesis techniques offer a sustainable alternative, minimizing toxic byproducts and enhancing the safety profile of nanoparticle production [34]. Indeed, many researchers have successfully embraced this green synthesis technique for CdS NPs synthesis. Botanical products like plant extracts, such as green tea [35], turmeric [36], or aloe vera [37] also many fungi [38], algae [39] and bacteria [40] have been used to synthesize nanoparticles. But here in this present work, we are using Arjuna Bark (Terminalia Arjuna) as the capping agent [41].

Arjuna, or Terminalia Arjuna has long held a significant position in Ayurvedic pharmacopoeia. Its bark has been used for millennia as a cardiotonic, lowering serum cholesterol, controlling hypertension, and treating a variety of cardiac conditions [42]. Arjuna bark is prized for its wide range of medicinal properties, which extend beyond cardiovascular support. These include strong anti-inflammatory and antioxidant properties, accelerated wound closure, altered digestive function, alleviation of respiratory conditions, and hepatic tissue protection. Additionally, new research suggests that it may have hypoglycemic effects, which could be advantageous for those with di-

 https://doi.org/10.54280/jse.255108

abetes [43]. We used Arjuna bark extract as a natural "capping" and reducing agent for the environmentally friendly manufacture of CdS nanoparticles in order to take advantage of its many beneficial qualities. In addition to removing the requirement for hazardous surfactants, using a plant-based capping reagent gives the surface of the nanoparticles biocompatible functional groups that could improve biological interactions. As a result, the key objective of this work is to synthesize CdS nanoparticles using Arjuna bark extract. This study's main objective is to thoroughly characterize the structural, optical, and antibacterial characteristics of the resultant particles, including crystallite size, band gap tuning, and photoluminescence behavior, as well as to assess the antibacterial efficacy. This work intends to develop sustainable production pathways and unlock multifunctional nanomaterials for biomedical and environmental applications by fusing traditional botanical knowledge with modern nanotechnology.

2 Sample preparation

2.1 Chemicals

The analytical grade $Cd(NO_3)_2$, $4H_2O$, and Na_2S were acquired from Loba Chemie Pvt. Ltd. (India) and were utilized without any additional purification. For capping and reducing purposes, the fresh bark of Terminalia Arjuna was collected from the garden of the Sainik School of Purulia district.

2.2 Preparation of Arjuna bark extract

The collected Arjuna bark was thoroughly washed with double distilled water to remove all the dirt particles. The bark was dried and ground using a pounder to make it finer. About 20 gm of this Arjuna bark was mixed with 200 ml DI water and kept at 60° in a heating mantle for an hour with constant stirring. After cooling down to room temperature, it was filtered using Whatman filter paper. The clean Brown extract of the Arjuna bark was stored in the refrigerator.

2.3 Synthesis of CdS nanoparticles

The synthesis of nanocrystalline CdS samples via chemical precipitation was conducted with different varying capping reagent concentrations. Cadmium nitrate $Cd(NO_3)_2$ and sodium sulfide (Na_2S) were used as the reactant materials and double distilled water was used as the solvent and Terminalia Arjuna bark extract was added as the capping reagent. The different concentrations of Arjuna extract were used in the different synthesized reactions. Five CdS samples Pure CdS, CdS-A, CdS-B, CdS-C and CdS-D were synthesized by using 0.00 ml, 5 ml, 10 ml, 15 ml, and 20 ml of Arjuna extract respectively. Initially, the 0.1 M $Cd(NO_3)_2$ and 0.1 M (Na_2S) dissolved in 100 ml double distilled water separately with vigorous magnetic stirring. The desired amount of Arjuna bark was also dissolved in $Cd(NO_3)_2$ the solution, and now this mixture was added to (Na_2S) solution, drop by drop with constant magnetic stirring. As soon as the reaction kicked off, the solution turned from clear to yellow. In the absence of light, the solution was vigorously stirred at a temperature range of 60-80° C for a duration of 19 hours [44]. The formation of CdS nano-colloids can be ascertained by the observation of the final color. This served as an indicator of the successful completion of the process. The prepared nano-colloids were carefully collected, washed thoroughly with water, and then filtered using Whiteman filter paper. This process ensures the highest level of precision and accuracy in the preparation of our nano-colloids. Finally, the assortments are dried in an open-air oven at 80° C and were ground into powder for further experimentation.

 https://doi.org/10.54280/jse.255108

2.4 Characterization of CdS nanoparticles

All of the samples were structurally analyzed using XRD and an X-ray diffractometer (PROTO AXRD) that operated with Cu-K radiation (0.154 nm). The data was obtained at a scanning rate of 0.5° per second at 600 watts over the angular range of the Bragg angle (2θ), which ranged from 20° to 70°. JASCO spectroscopy (Model No: 4700) was been employed for Fourier Transmission Infrared Spectroscopy (FTIR). For optical characterization, the UV–Vis spectroscopic approach was used through a JASCO V-630 two-beam spectrophotometer in the range of 350–580 nm at room temperature. In addition, photoluminescence spectroscopy (PL) was performed with an Agilent Cary Eclipse fluorescence spectrometer to study the PL spectra at excitation wavelengths of 280 nm and 400 nm, with a 10 nm interval. Raman spectroscopy observations were performed using a Renishaw InVia Raman microscope equipped with a solid-state laser source with a laser power of 1% of 50 mW and an excitation wavelength of 532 nm.

3 Results and discussion

3.1 Study of X-ray diffractograms (XRD)

The X-ray diffraction spectrum of as-prepared CdS samples is shown in Figure 1. The peak position of XRD patterns were obtained at 2θ values of pure CdS, CdS-A, CdS-B, CdS-C, CdS-D NPs at 26.57°, 43.78°, and 51.92° which correspond to (111), (220), and (311) planes, respectively [44]. The data collected indicate the presence of a cubic structure in all the samples investigated (JCPDS no: 10-0454) [44].

The crystallite size of CdS nanoparticles was determined using the well-known Debye-Scherer's equation [45-46]

$$D = \frac{0.94\lambda}{\beta \cos\theta} \tag{1}$$

where D is the crystallite size, λ is the wavelength of Cu-K_α (0.154 nm), β represents the FWHM of the diffraction peak in radians, and θ is the Bragg's diffraction angle. The estimated crystallite sizes are 4.35 nm, 4.47 nm, 4.48 nm, 4.63 nm and 4.75 nm for the synthesized pure CdS, and CdS-A, CdS-B, CdS-C, CdS-D samples, respectively. It has been noted that, the calculated average crystallite size values are increased from 4.35 to 4.75 nm. The possible reason for this increment of average crystalline size may be attributed to the introduction of Arjuna extract, which may alter the nucleation and growth kinetics, leading to increased crystalline size. Also, it is noteworthy that the amount of doping of bio extract increases the crystalline size.

3.2 FTIR analysis

A FTIR spectroscopy study was carried out to determine the molecular structure of synthesized compounds and identify the functional groups present in them. Figure 2 shows the FTIR transmission spectra of all synthesized samples in the range 500-4000 cm^{-1}. In all samples, spectral profiles were identical with minor band position shifts.

The FTIR spectra of all synthesized CdS NPs exhibit a band around 996-1222 cm^{-1} is attributed to the C-O stretching vibration, and 1369 cm^{-1} is assigned to the wagging vibration of CH_2. In the IR spectra [47], the signature of =C=O functional groups in carbonyls, carboxyls or carboxylic anhydrides is evident at about 1742 cm^{-1} [48]. The observed band around 2362 cm^{-1} is assigned to the C-H stretch [49]. Proteins can bind to CdS NPs either through free amine groups or cysteine residues present in the Arjuna extract [50].

 https://doi.org/10.54280/jse.255108

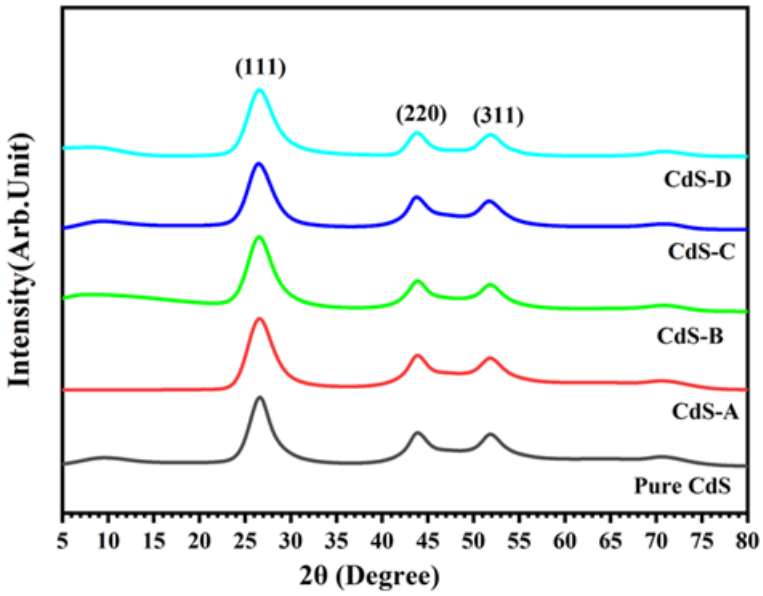

Figure 1: XRD patterns of all the synthesized CdS NPs.

Thus, the FTIR data analysis indicates the formation of CdS nanoparticles and the presence of protein molecules in the Arjuna bark extract which creates the binding of CdS NPs [50].

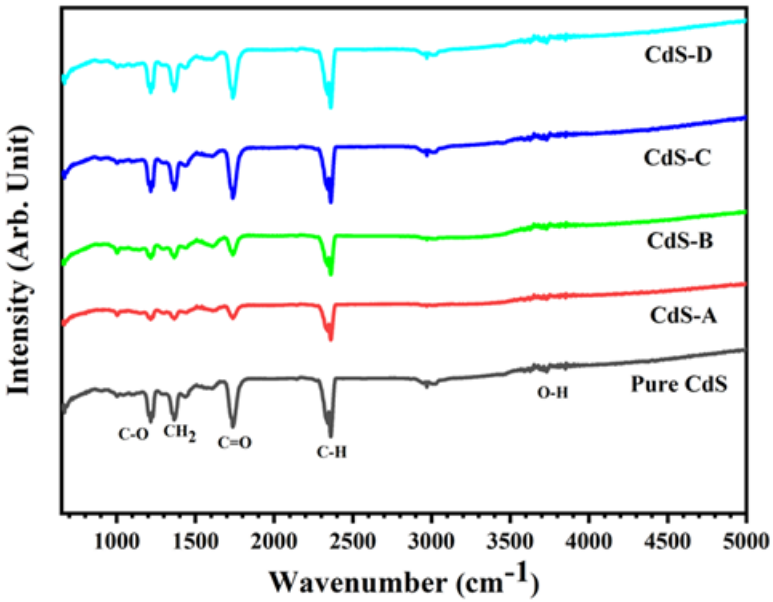

Figure 2: The FTIR spectra of CdS samples.

3.3 Raman analysis

The Raman spectra of room-temperature CdS nanoparticles are depicted in Figure 3, providing important information on their structural and vibrational characteristics. Near 306 cm^{-1}, a strong peak is seen, corresponding to the CdS crystal lattice's first-order longitudinal optical (LO) phonon mode. This Raman band's clarity and symmetry clearly show that the

 https://doi.org/10.54280/jse.255108

produced nanoparticles have a high degree of crystallinity, few structural distortions, and very little input from secondary phases or impurities [51]. It may be mentioned that the first-order longitudinal optical phonon vibration (1 LO) in the crystal lattice provides information about lattice dynamics, plasmon-phonon coupling and structural quality. It's interesting to note that the LO phonon peak noticeably shifts towards lower wavenumbers (redshift) in several CdS samples. This spectral behaviour points to minor but noteworthy changes in the nanoparticles' lattice dynamics. The phonon confinement effect, which intensifies with decreasing particle size, is responsible for such shifts.

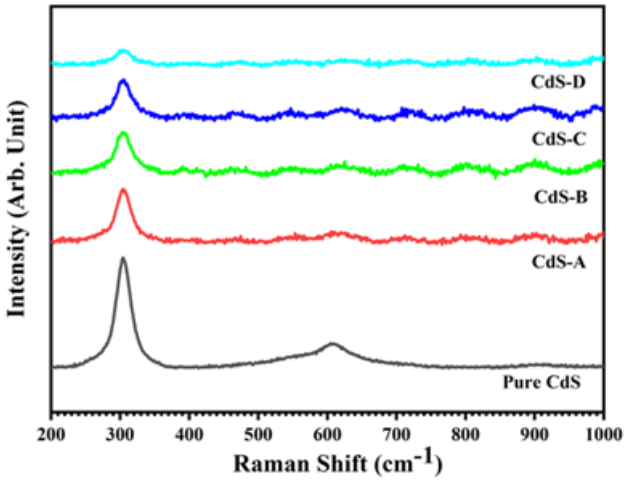

Figure 3: Raman Spectra of studied samples.

Peak broadening or shifting results from the relaxation of the Raman selection rules caused by the spatial restriction of phonons in nanoscale materials [52]. Furthermore, our observations did not reveal the peaks that would be predicted in hexagonal CdS, confirming that the CdS microspheres have the zinc-blende cubic structure. Additionally, Figure 3 demonstrates that as the ratio of Arjuna extract increases, the peak intensity decreases. The larger grain size of CdS nanoparticle is responsible for this declining intensity, and these findings are in good agreement with the XRD data.

3.4 Optical study

3.4.1 Study of absorbance spectra

By studying optically induced transitions and determining the optical band gap energy of the materials under consideration, optical absorption spectra are useful for studying structural changes. The wavelength dependence of absorption spectra for five samples Pure CdS, CdS-A, CdS-B, CdS-C, and CdS-D are presented in Figure 4, which also shows the UV-visible spectra of these samples. Figure 4 is the UV–Visible absorbance spectra of pure CdS nanoparticles and extract- mediated CdS nanoparticles (CdS-A, CdS-B, CdS-C, CdS-D) in the 200–600 nm wavelength range. Pure CdS nanoparticles (black line) have comparatively weak absorbance without a clear excitonic peak, indicating larger particle size and potential aggregation that causes low optical activity. Conversely, the capping by extracts of CdS materials exhibits greatly increased absorbance over the UV–visible range, which validates the function of phytochemicals to enhance nucleation, stability, and surface passivation. The extract-capped CdS samples

 https://doi.org/10.54280/jse.255108

(CdS-A, CdS-B, CdS-C, and CdS-D) are exhibited enhanced absorption peaks and a noticeable blue-shift in the absorption edge, which suggests that the phytochemicals in the leaf extract have decreased particle size and improved surface passivation. The blue-shift observed in the capped samples has been explained by the quantum confinement effect, which increases the optical band gap when the particle size grows or decreases less than the exciton Bohr radius [53]. A blue-shift in absorption edge is distinctly noted in extract-capped CdS over pure CdS, establishing the quantum confinement effect due to the decrease in crystallite size. In this context it should be mentioned that the quantum confinement is known as the phenomenon that occurs when the particle size becomes comparable to or smaller than the exciton Bohr radius, leading to discrete energy levels and size-dependent optical properties. These findings indicate that biomolecule-assisted synthesis not only enhances absorbance properties but also improves the material's performance for optoelectronic and photocatalytic purposes by broadening the window of absorption and inhibiting recombination losses.

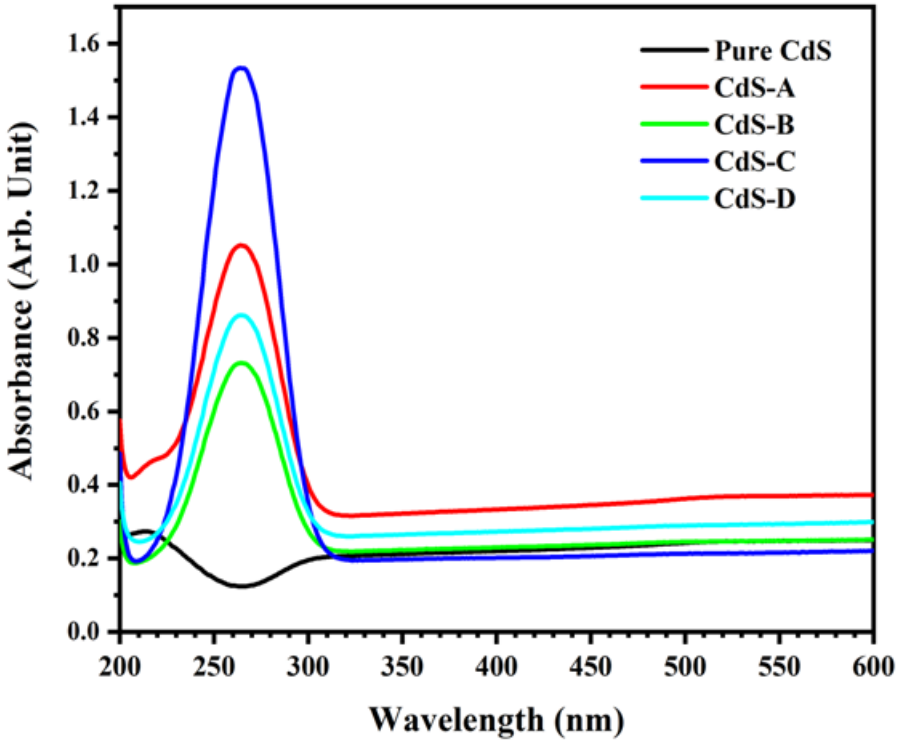

Figure 4: Absorbance spectra of CdS samples.

3.4.2 Study of energy bandgap

It is important to inspect the optical band gap energy of a material to determine its semiconducting properties. To estimate the optical band gap energy of the samples under study, Tauc plot was used. According to Figure 5, the band gap energy reduces from 4.49 eV to 3.82 eV as the doping concentration increases. Band gap values of CdS were reported in earlier studies can be explained by changes in crystallite size [54].

 https://doi.org/10.54280/jse.255108

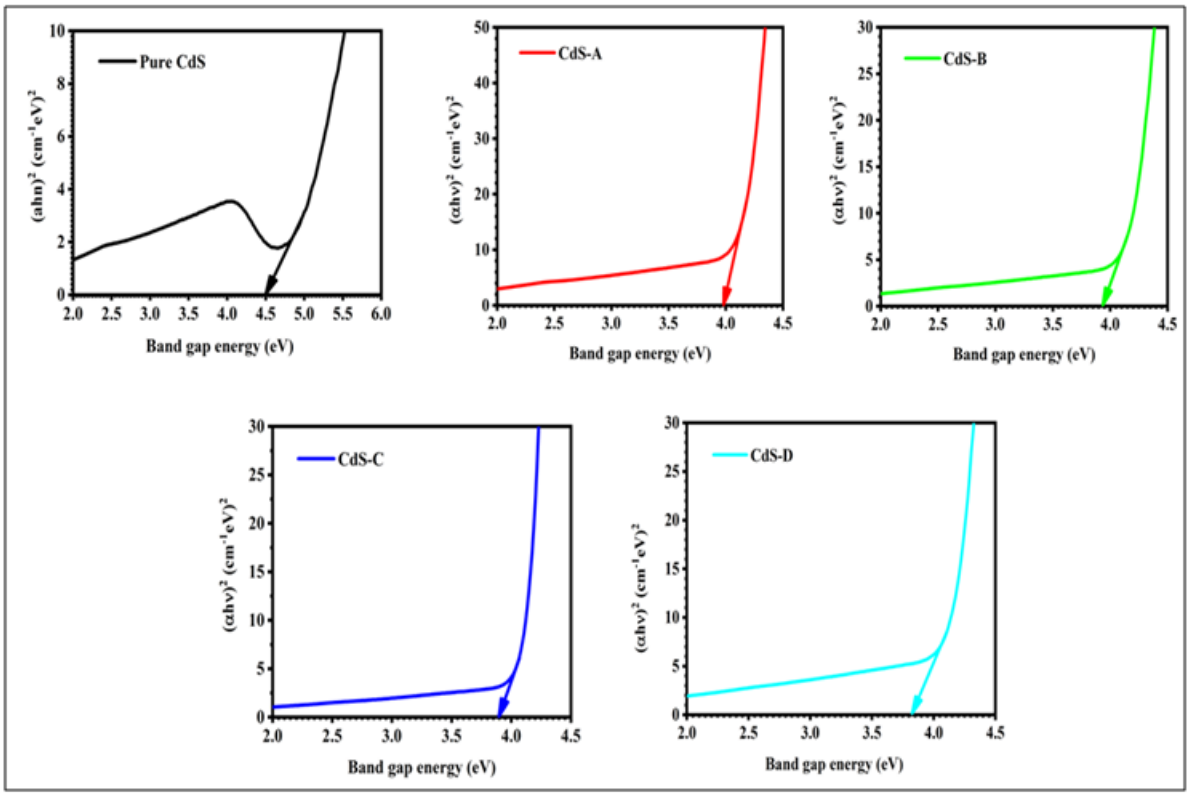

Figure 5: Tauc Plot of synthesized bio-capped CdS nanoparticles.

3.5 Photoluminescence study

The as-synthesised CdS nanocrystals' emissive behaviour was clarified using photoluminescence (PL) spectroscopy. The room temperature PL spectra, which span the 425–600 nm range, are shown in Figure 6 under 400 nm excitation. Every specimen has two prominent, sharply defined bands that are centred at around 488 and 535 nm, respectively. Radiative recombination involving inherent lattice defects, like sulphur vacancies or surface dangling bonds, which introduce defect levels slightly below the conduction band, is typically attributed with the higher energy feature at 488 nm (≈2.54 eV) [55].

Group II–VI semiconductors are known for this defect-related emission, which frequently acts as an optical fingerprint of the surface chemistry and crystal quality. In contrast, band edge or 'short lifetime' excitonic emission is responsible for the lower energy band around 483 nm, which becomes more noticeable as particle size increases significantly. In contrast to bulk CdS, quantum confinement effects increase the degeneracy of the electronic sub bands, hence expanding the effective band gap and causing the emission to shift slightly towards shorter wavelengths (blue shift). From an application perspective, visible light optoelectronic technologies greatly benefit from the strong output at (520-545 nm). In particular, size tunable CdS nanocrystals are attractive active layers in light emitting diodes, laser diodes, and photonic sensors where narrow band, high intensity emission is required [56]. Furthermore, the coexistence of band edge and defect state luminescence offers a convenient platform for engineering broad spectrum emitters through judicious surface passivation or core shell construction. Overall, the PL signatures confirm both the nanoscale dimensions and the defect state of the prepared CdS samples, validating their suitability for advanced optoelectronic applications.

 https://doi.org/10.54280/jse.255108

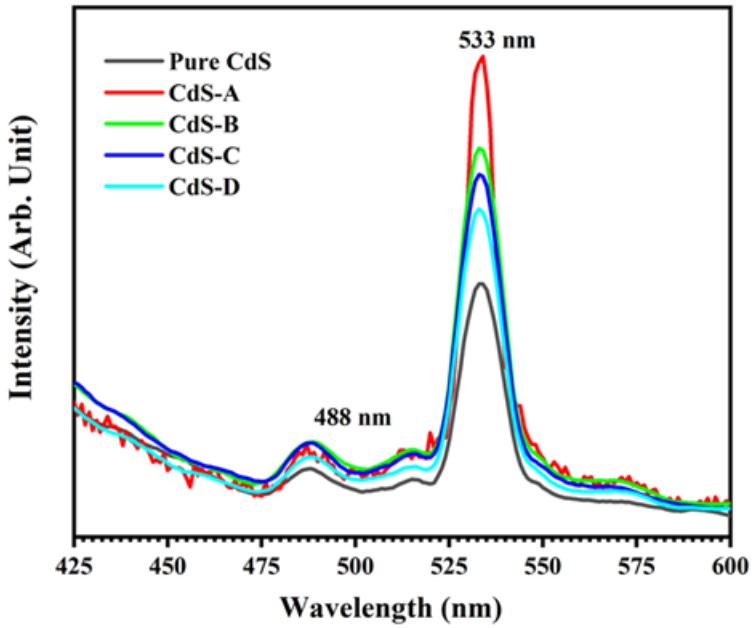

Figure 6: Photoluminescence spectra of the studied sample.

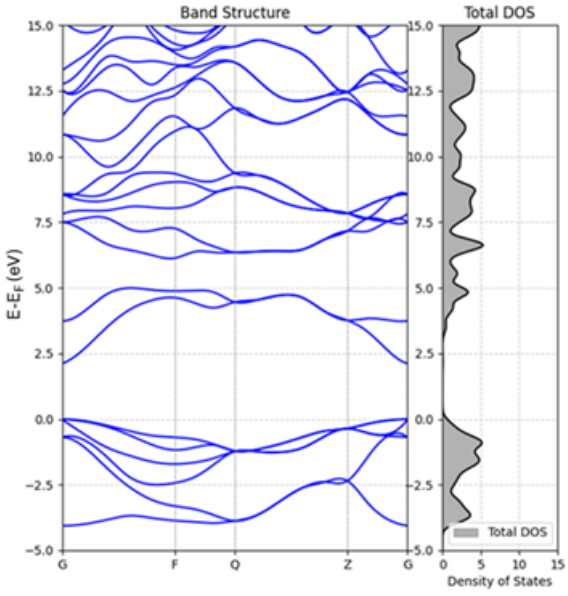

Figure 7: DFT- calculated band structure (left) and total density of states (DOS, right) of CdS.

4 DFT study

To complement the experimental characterization, density functional theory (DFT) calculations were performed to investigate the electronic band structure and density of states (DOS) of CdS. The computed band structure along high symmetry points (G–F–Q–Z–G) is shown in Figure 7. The results reveal a direct band gap at the Γ-point, consistent with the known semiconducting behavior of CdS. The calculated band gap is approximately ∼2.2–2.4 eV, which agrees well with the experimentally obtained optical band gap values (4.49-3.82 eV) from the Tauc plots (Figure 5). The slight underestimation of the band gap is expected, as generalized gradi-

 https://doi.org/10.54280/jse.255108

ent approximation (GGA) functionals typically underestimate electronic band gaps.

5 Conclusion

The work describes the use of Arjuna bark as a capping agent in the synthesis of CdS nanoparticles utilizing a green chemical technique. The cubic structure was revealed by XRD measurements. Furthermore, the band gap of the synthesized CdS NPs were estimated through UV-visible spectra, and are found to decrease from 4.49 eV to 3.82 eV with different Arjuna bark extract concentrations. The outcomes of the DFT study agree with the experimentally obtained band gap values and provide an understanding of the electronic structure of the synthesized CdS nanoparticles. The room temperature UV–Visible absorption spectra reveal the particle size dependent absorption edge. The XRD results indicate that the particles get larger sizes on increasing capping reagent concentration. On increasing the capping reagent concentration, the 1LO peak position in Raman spectra is slightly shifted towards higher wavenumber as the particle size gets larger and peak gets progressively broader. PL study attributes a decrement of the peak intensity due to interstitial sulphur with increasing capping reagent concentration.

Acknowledgements

We are grateful to Sidho-Kanho-Birsha University, Purulia for providing the essential infrastructural facility. S. Mondal acknowledges the financial assistance from the Department of Science & Technology-Fund for Improvement of Science & Technology Infrastructure (SR/FST/PS-1/2020/159) New Delhi, India, and the RUSA grant of SKBU and the Research Award Grant to promote faculty research (2025-2029), Sidho-Kanho-Birsha University.

References

[1] Pandit, C., Roy, A., Ghotekar, S., Khusro, A., Islam, M. N., Emran, T. B., Lam, S. E., Khandaker, M. U., & Bradley, D. A. (2022). Biological agents for synthesis of nanoparticles and their applications. *Journal of King Saud University – Science*, 34, 101869.

[2] Khan, Y., Sadia, H., Ali Shah, S. Z., Khan, M. N., Shah, A. A., Ullah, N., Ullah, M. F., Bibi, H., Bafakeeh, O. T., Khedher, N. B., Eldin, S. M., Fadh, B. M., & Khan, M. I. (2022). Classification, synthetic, and characterization approaches to nanoparticles and their applications in various fields of nanotechnology: A review. *Catalysts*, 12, 1386.

[3] Baig, N., Kammakakam, I., & Falath, W. (2021). Nanomaterials: A review of synthesis methods, properties, recent progress, and challenges. *Materials Advances*, 2, 1821–1871.

[4] Bayda, S., Adeel, M., Tuccinardi, T., Cordani, M., & Rizzolio, F. (2020). The history of nanoscience and nanotechnology: From chemical–physical applications to nanomedicine. *Molecules*, 25, 112.

[5] Hadi, I. H., Khashan, K. S., & Sulaiman, D. (2021). Cadmium sulphide (CdS) nanoparticles: Preparation and characterization. *Materials Today: Proceedings*, 42, 3054–3056.

[6] Aruna Devi, R., Latha, M., Velumani, S., Oza, G., Reyes-Figueroa, P., Rohini, M., Becerril-Juarez, I. G., Lee, J. H., & Yi, J. (2015). Synthesis and characterization of cadmium sulfide nanoparticles by chemical precipitation method. *Journal of Nanoscience and Nanotechnology*, 15, 8434–8439.

[7] Dabhane, H., Ghotekar, S., Tambade, P., Pansambal, S., Murthy, H. C. A., Oza, R., & Medhane, V. (2021). A review on environmentally benevolent synthesis of CdS nanoparticle and their applications. *Environmental Chemistry and Ecotoxicology*, 3, 209–230.

[8] Sahu, M. K. (2019). Semiconductor nanoparticles theory and applications. *International Journal of Applied Engineering Research*, 14, 491–494.

[9] Hossain, N., Mobarak, M. H., Mimona, M. A., Islam, M. A., Hossain, A., Zohura, F. T., & Chowdhury, M. A. (2023). Advances and significances of nanoparticles in semiconductor applications – A review. *Materials Science in Semiconductor Processing*, 138, 106307.

[10] Hussein, H. S. (2023). The state of the art of nanomaterials and its applications in energy saving. *Bulletin of the National Research Centre*, 47, 7.

 https://doi.org/10.54280/jse.255108

[11] Christian, F., Edith, S., Selly, D., Adityawarman, D., & Indarto, A. (2013). Application of nanotechnologies in the energy sector: A brief and short review. *Frontiers in Energy*, 7, 6–18.

[12] Ghasemzadeh, F., & Shayan, M. E. (2020). Nanotechnology in the service of solar energy systems.

[13] Wang, L., Teles, M. P. R., Arabkoohsar, A., Yu, H., Ismail, K. A. R., Mahian, O., & Wongwises, S. (2022). A holistic and state-of-the-art review of nanotechnology in solar cells. *Sustainable Energy Technologies and Assessments*, 54, 102864.

[14] Sethi, V. K., Pandey, M., & Shukla, P. (2011). Use of nanotechnology in solar PV cell. *International Journal of Chemical Engineering and Applications*, 2.

[15] Nguyen, H. P. T., Arafin, S., Piao, J., & Cuong, T. V. (2016). Nanostructured optoelectronics: Materials and devices. *Journal of Nanomaterials*.

[16] Mazayen, Z. M., Ghoneim, A. M., Elbatanony, R. S., Basalious, E. B., & Bendas, E. R. (2022). Pharmaceutical nanotechnology: From the bench to the market. *Future Journal of Pharmaceutical Sciences*, 8.

[17] Rizvi, S. A. A., & Saleh, A. M. (2018). Applications of nanoparticle systems in drug delivery technology. *Saudi Pharmaceutical Journal*, 26, 64–70.

[18] Sharma, D., & Hussain, C. M. (2020). Smart nanomaterials in pharmaceutical analysis. *Arabian Journal of Chemistry*, 13, 3319–3343.

[19] Huang, X., Zhu, Y., & Kianfar, E. (2021). Nano biosensors: Properties, applications and electrochemical techniques. *Journal of Materials Research and Technology*, 12, 1649–1672.

[20] Ramesh, M., Janani, R., Deepa, C., & Rajeshkumar, L. (2023). Nanotechnology-enabled biosensors: Fundamentals, design principles, materials, and applications. *Biosensors*, 13, 40.

[21] Pandit, S., Dasgupta, D., Dewan, N., & Ahmed, P. (2016). Nanotechnology based biosensors and its application. *The Pharma Innovation*, 5, 18–25.

[22] Touhami, A. (2014). *Biosensors and nanobiosensors: Design and applications*. One Central Press.

[23] Holzinger, M., Le Goff, A., & Cosnier, S. (2014). Nanomaterials for biosensing applications: A review. *Analytical Chemistry*, 2.

[24] Khandel, P., Yadaw, R. K., Soni, D. K., Kanwar, L., & Shah, S. K. (2018). Biogenesis of metal nanoparticles and their pharmacological applications: Present status and application prospects. *Journal of Nanostructure Chemistry*, 8, 217–254.

[25] Yaqoob, A. A., Ahmad, H., Parveen, T., Ahmad, A., Oves, M., Ismail, I. M. I., Qari, H. A., Umar, K.,& Ibrahim, M. N. M. (2020). Recent advances in metal decorated nanomaterials and their various biological applications: A review. *Nanoscience*, 8.

[26] Klebowski, B., Depciuch, J., Parlinska-Wojtan, M., & Baran, J. (2018). Applications of noble metal-based nanoparticles in medicine. *International Journal of Molecular Sciences*, 19, 4031.

[27] Miskin, C. K., Deshmukh, S. D., Vasiraju, V., Bock, K., Mittal, G., Dubois-Camacho, A., Vaddiraju, S., & Agrawal, R. (2019). Lead chalcogenide nanoparticles and their size-controlled self-assemblies for thermoelectric and photovoltaic applications. *ACS Applied Nano Materials*, 2, 1242–1252.

[28] Feng, Y., Marusak, K. E., You, L., & Zauscher, S. (2018). Biosynthetic transition metal chalcogenide semiconductor nanoparticles: Progress in synthesis, property control and applications. *Current Opinion in Colloid & Interface Science*, 38, 190–203.

[29] Olawale, F., Oladimeji, O., Ariatti, M., & Singh, M. (2022). Emerging roles of green-synthesized chalcogen and chalcogenide nanoparticles in cancer theranostics. *Journal of Nanotechnology*.

[30] Oladeji, I. O., & Chow, L. (2005). Synthesis and processing of CdS/ZnS multilayer films for solar cell application. *Thin Solid Films*, 474, 77–83.

[31] Soleimani, F., & Nezamzadeh-Ejhieh, A. (2020). Photocatalytic activity of CdSe–ZnS nanocomposite in the photodegradation of rifampin in aqueous solution. *Journal of Materials Research and Technology*, 9, 16237–16251.

[32] Rodríguez-Mas, F., Ferrer, J. C., Alonso, J. L., & de Ávila, S. F. (2019). Expanded electroluminescence in high load CdS nanocrystals PVK-based LEDs. *Nanomaterials*, 9.

 https://doi.org/10.54280/jse.255108

[33] Chopra, H., Bibi, S., Singh, I., Hasan, M. M., Khan, M. S., Yousafi, Q., Baig, A. A., Rahman, M. M., Islam, F., Emran, T. B., & Cavalu, S. (2022). Green metallic nanoparticles: Biosynthesis to applications. *Frontiers in Bioengineering and Biotechnology*, 10.

[34] Ying, S., Guan, Z., Ofoegbu, P. C., Clubb, P., Rico, C., He, F., & Hong, J. (2022). Green synthesis of nanoparticles: Current developments and limitations. *Environmental Technology & Innovation*, 26.

[35] G., K. S. V. (2017). Green synthesis of iron nanoparticles using green tea leaves extract. *Journal of Nanomedicine & Biotherapeutic Discovery*, 7.

[36] Alsammarraie, F. K., Wang, W., Zhou, P., Mustapha, A., & Lin, M. (2018). Green synthesis of silver nanoparticles using turmeric extracts and investigation of their antibacterial activities. *Colloids and Surfaces B: Biointerfaces*, 171, 398–405.

[37] Tippayawat, P., Phromviyo, N., Boueroy, P., & Chompoosor, A. (2016). Green synthesis of silver nanoparticles in *Aloe vera* extract prepared by a hydrothermal method and their synergistic antibacterial activity. *PeerJ*.

[38] Wang, D., Xue, B., Wang, L., Zhang, Y., Liu, L., & Zhou, Y. (2021). Fungus-mediated green synthesis of nanosilver using *Aspergillus sydowii* and its antifungal/antiproliferative activities. *Scientific Reports*, 11.

[39] Chugh, D., Viswamalya, V. S., & Das, B. (2021). Green synthesis of silver nanoparticles with algae and the importance of capping agents in the process. *Journal of Genetic Engineering and Biotechnology*, 19.

[40] Bahrulolum, H., Nooraei, S., Javanshir, N., Tarrahimofrad, H., Mirbagheri, V. S., Easton, A. J., & Ahmadian, G. (2021). Green synthesis of metal nanoparticles using microorganisms and their application in the agrifood sector. *Journal of Nanobiotechnology*, 19.

[41] Raj, S., Singh, H., Trivedi, R., & Soni, V. (2020). Biogenic synthesis of AgNPs employing *Terminalia arjuna* leaf extract and its efficacy toward catalytic degradation of organic dyes. *Scientific Reports*, 10.

[42] Dwivedi, S., & Chopra, D. (2014). Revisiting *Terminalia arjuna* – An ancient cardiovascular drug. *Journal of Traditional and Complementary Medicine*, 4, 224–231.

[43] Thomson, H. A. J., Ojo, O. O., Flatt, P. R., & Abdel-Wahab, Y. H. A. (2014). Aqueous bark extracts of *Terminalia arjuna* stimulate insulin release and enhance insulin action. *Austin Journal of Endocrinology and Diabetes*, 1.

[44] Zhou, G. J., Li, S. H., Zhang, Y. C., & Fu, Y. Z. (2014). Biosynthesis of CdS nanoparticles in banana peel extract. *Journal of Nanoscience and Nanotechnology*, 14, 4437–4442.

[45] Pathania, D., Sarita, S., & Rathore, B. S. (2011). Synthesis, characterization and photocatalytic application of bovine serum albumin capped cadmium sulphide nanoparticles. *Chalcogenide Letters*, 8, 396–404.

[46] Reddy, P. L., Deshmukh, K., Kovářík, T., Nambiraj, N. A., & Shaik, K. P. (2020). Green chemistry mediated synthesis of cadmium sulphide/polyvinyl alcohol nanocomposites: Assessment of microstructural, thermal, and dielectric properties. *Polymer Composites*, 41, 2054–2067.

[47] Tudu, P., Mondal, R., Santra, S., Kuiri, B., Biswas, D., Kabi, S., Uddin, M. M., Chowdhury, S., Patra, A. S., & Mondal, S. (2024). Annealing effect on structural and optical properties of green-synthesized CdS nanoparticles: A comparative study. *MRS Advances*, 9, 1–8.

[48] Li, C., Tang, Y., Yao, K., Zhou, F., Ma, Q., Lin, H., Tao, M., & Liang, J. (2006). Decoration of multiwall nanotubes with cadmium sulfide nanoparticles. *Carbon*, 44, 2021–2026.

[49] Halliday, D., Resnick, R., & Walker, J. (2011). *Fundamentals of physics* (9th ed.). Wiley.

[50] Ashcroft, N. W., & Mermin, N. D. (1976). *Solid state physics*. Saunders College Publishing.

[51] Xiong, S., Xi, B., Wang, C., Zou, G., Fei, L., Wang, W., & Qian, Y. (2007). Shape-controlled synthesis of 3D and 1D structures of CdS in a binary solution with L-cysteine's assistance. *Chemistry – A European Journal*, 13, 3076–3081.

[52] Rengaraj, S., Jee, S. H., Venkataraj, S., Kim, Y., Vijayalakshmi, S., Repo, E., Koistinen, A., & Sillanpää, M. (2011). *Journal of Nanoscience and Nanotechnology*, 11, 1–10.

 https://doi.org/10.54280/jse.255108

[53] Murray, C. B., Norris, D. J., & Bawendi, M. G. (1993). Synthesis and characterization of nearly monodisperse CdE (E = S, Se, Te) semiconductor nanocrystallites. *Journal of the American Chemical Society*, 115, 8706–8715.

[54] Tauc, J. (1972). Optical properties of solids. In F. Abeles (Ed.), *Optical properties of solids* (pp. 277–310). North Holland.

[55] Goto, F., Shirai, K., & Ichimura, M. (1998). Defect reduction in electrochemically deposited CdS thin films by annealing in O_2. *Solar Energy Materials and Solar Cells*, 50, 147–153.

[56] Lavanya, T., & Jaya, N. V. (2011). Synthesis and characterization of pure CdS nanoparticles for optoelectronic applications. *Transactions of the Indian Ceramic Society*, 70, 119–123.

 https://doi.org/10.54280/jse.255108